Forestry An International Journal of Forest Research

Institute of Chartered Foresters

Forestry 2023; **96**, 155–169, https://doi.org/10.1093/forestry/cpac053
Advance Access publication 17 December 2022

Challenges in automatic forest change reporting through land cover mapping

Laura Alonso[1,*], Andrés Rodríguez[1], Juan Picos[1] and Julia Armesto[1,2]

[1]*Engineering of Natural Resources and Environment, Forestry Engineering School, University of Vigo – A Xunqueira Campus, Pontevedra 36005, Spain*
[2]*CINTECX, GESSMin Group (Safe and Sustainable Management of Mineral Resources), Vigo 36310, Spain*

*Corresponding author E-mail: laura.alonso.martinez@uvigo.es

Received 27 May 2022

Up-to-date knowledge about changes in forest resources and their spatial distribution is essential for sustainable forest management. Therefore, monitoring of forest evolution is increasingly demanded by national and international agencies to design forestry policies and to track their progress. Annually updated land cover maps based on open access satellite imagery may serve as a primary tool for monitoring forest surface evolution over time. Spatially detailed information about forest change might be obtained by comparing land cover maps over time. This study aims to better understand the processes underlying pixels whose land cover changes from 1 year's map to the next and to understand why errors occur. In this study, two annual land cover maps were produced using Sentinel-2 images and afterwards they were compared. The comparison was performed in terms of total surface occupied in each map by each of the classes (net comparison) and in terms of spatial agreement, comparing the results pixel to pixel. The study was performed for the entire region of Galicia (in the Northwest of Spain) for the years 2019 and 2020. Land cover maps obtained had overall accuracies of 82 and 85 per cent. Differences in the total surface of change were encountered when performing the net comparison and spatial agreement comparison. The detailed analysis performed in this study helps to better understand the processes underlying the maps' discrepancies revealing the processes leading to wrongly identified forest changes. Future studies could aim to integrate this knowledge into the monitoring system to improve the ultimate usability of land cover maps to retrieve information about forest changes.

Introduction

An increasing interest in developing adequate policies for sustainable forest management is arising given the current context of climate change, and due to the essential role that forests play in its mitigation (Pan, 2011). The efficiency of sustainable forest management policies depends greatly on having a detailed understanding of the distribution of forest resources and their evolution (FAO, 2020). Updated land use maps depicting the forest area of a region constitute useful tools for forest managers when it comes to policy design, planning and implementation and for efficiency evaluation. Along these lines, one of the main pillars of the FAO's REDD++ program (Food and Agriculture Organization of the United Nations, Reducing Emissions from Deforestation and forest Degradation, plus the sustainable management of forests, and the conservation and enhancement of forest carbon stocks) to encourage developing countries to contribute to climate change mitigation, is providing forest monitoring tools (FAO, 2021). Reliable and updated information is also needed to design any policies aimed at achieving the forest-related goals included in the United Nations 2030 Agenda (United Nations, 2021) and in the Paris Agreement (European Commission, 2021), as well as to monitor and report different countries' progress towards achieving these goals. Therefore, there is an increasing demand from national and international agencies for information about forests' distribution and changes.

Open-access satellite data are one of the most important sources of information for monitoring the evolution of forest area at a large scale (Wulder *et al*., 2018; World Resources Institute, 2022). In fact, one of the strategies followed by multiple national and international agencies to track forest evolution is the automatic production of land cover maps which can be frequently updated using satellite data and which are oriented towards specific information needs (Inglada *et al*., 2017; Mundialis, 2019; UKCEH, 2020; Junta de Castilla y León, 2021; S2GLC, 2021). Once land cover maps are obtained for regular intervals of time, comparing them can be useful for studying the evolution over time of specific land cover classes of interest, for example forest area. Forest change estimations can also be derived from these maps (Wickham *et al*., 2014; Gilani *et al*., 2020; Ji *et al*., 2021).

Handling Editor: Dr. Fabian Fassnacht

However, several concerns exist when performing comparisons of maps from consecutive years. A simple direct comparison may lead to an inconsistent change report (Congalton *et al*., 2014; Palahí *et al*., 2021). First, it is essential to ensure that all the maps compared were created using the same methodology (Congalton *et al*., 2014; Kang *et al*., 2020; Palahí *et al*., 2021). Second, the comparison of maps from consecutive years must consider that each map may have class-specific errors with the potential to blur the conclusions related to changes. This is because pixels that are assigned to a different land cover in an updated map with respect to the earlier map might not necessarily correspond unequivocally to true areas of change. Therefore, quantifying the area of forest change cannot be accomplished simply by quantifying the pixels that have changed; rather, the area of uncertainty must be quantified as well (Olofsson *et al*., 2013). Another important concern is the regular presence of spurious changes, i.e. changes that cannot possibly have occurred within the study period. For example, a pixel may be classified as a certain tree cover (i.e. Conifers) in one land cover map, and as a contradicting tree cover (i.e. Broadleaves) in the land cover map from the next year. Depending on the scale and on the particularities of the study area, the strategy for dealing with spurious changes may differ and hence this topic must be studied in detail (Abercrombie and Friedl, 2015; Zhu *et al*., 2020). In addition, if the focus is on studying the evolution of forests over time, it is important to find a way to deal with harvested areas. They may be assigned to non-tree-cover classes at the time directly following the harvest, but may still be considered forest areas according to official definitions of forest areas. Multitemporal analysis may hence be required to correctly label stands that were logged during forest area estimations (FAO, 2018; Wulder *et al*., 2020).

Given the considerations involved in the comparison of consecutive-year land cover maps, it is essential to analyze them in detail in every region of interest (Jin *et al*., 2017). Producing consecutive-year land cover maps with the aim of monitoring forested areas can be especially challenging in areas with a high level of stand fragmentation and a high harvesting rate. In such regions, harvesting areas may be small and difficult to identify when comparing the land cover maps before and after an intervention. A great number of edge pixels with mixed spectral signatures may also potentially be labeled as change pixels when performing the map comparison. These edge effects generate noise that complicates the identification of real changes (Kussul *et al*., 2016).

This study analyses the implications and challenges of comparing annual land cover maps produced by supervised classification of Sentinel-2 images. The geographic focus of the study is Galicia, a region in the Northwest of Spain characterized by a high level of forest stand fragmentation and a high rate of harvesting. Two land cover maps were produced in consecutive years and compared to detect forest cover changes. They were compared in terms of total surface occupied in each map by each of the classes. In addition, a detailed spatial comparison using a pixel to pixel analysis was performed. These analyses aim to understand the underlying processes behind the pixels' land cover changes from one map to the next as well as to identify which factors can lead to the misidentification of change. This can help to improve the monitoring of forests using consecutive land cover classifications, especially in areas with a highly active forest sector or where there is a dominance of species with short rotation periods, and/or high stand fragmentation.

Study area

The study area corresponds to the whole region of Galicia (Northwest of Spain) (see Figure 1). It comprises a total of 29.575 km^2. Forty-eight per cent of its surface area is covered by forest (canopy cover $\geq$10 per cent) (de Galicia, 2016). The main Galician forests are: productive forests of mainly *Eucalyptus* spp., *Pinus pinaster*, *Pinus radiata* and *Pinus sylvestris*, broadleaf mixed forests (*Quercus* spp., *Castanea sativa*, etc.) and riparian forests (de Galicia, 2016). Galicia has both Atlantic and Mediterranean climates (Meteogalicia, 2021). The climate variability and the tree species diversity of Galicia translate into diverse starting and ending points of the phenological period depending on the tree location and species (Sánchez *et al*., 2013).

Galicia has an extremely active forestry sector (Levers *et al*., 2014; MITERD, 2018), 50 per cent of the volume of timber annually harvested in Spain is harvested in Galicia. The official harvesting records for the last 6 years (2015–2020) report a mean value of 88 140 administrative harvesting requests per year (de Galicia, 2021). In addition, Eucalyptus plantations may represent a challenge in terms of monitoring due to their short rotation cycles (between 12 and 15 years) (Tolosana *et al*., 2017; Arenas *et al*., 2019). In addition, the forest stands in Galicia are highly fragmented, mainly due to the great degree of land fragmentation attributed to the great number of land owners that possess small forest parcels, some of which have had agricultural uses in earlier times. It is estimated that ~40 per cent of the productive forest area corresponds to parcels smaller than 0.5 ha (Spanish government, 2011).

Materials

Satellite images

A set of Sentinel-2 images was used in this study. The Sentinel-2 constellation was launched as a part of the European Copernicus program to monitor the Earth's land surface and, in particular, its vegetation (ESA, 2015a). The Sentinel-2 constellation (ESA, 2015b) has two satellites equipped with a medium-resolution multispectral instrument (MSI-12 bits) with 13 spectral bands. The bands' spatial resolutions range from 10 to 60 m. A detailed description of the Sentinel-2 bands is presented in Table 1.

The constellation allows for a revisit time of 5 days or less. The Sentinel-2 product used in this study was the Level 2A product, which has undergone geometric, radiometric and atmospheric corrections. For each of the seven Sentinel-2 tiles corresponding to Galicia, a time series of images corresponding to the 2 study years 2019 and 2020 was downloaded from the Copernicus Open Access Hub (ESA, 2021). Each set is a compound of 12 Sentinel-2 images, with one image per month to account for all of the phenological stages of the vegetation. Images were selected using the criteria described in Alonso *et al*. (2021). For each month, the image with the least cloud cover was selected, with the maximum threshold being 50 per cent. In cases where no image with < 50 per cent cloud cover was available for a specific

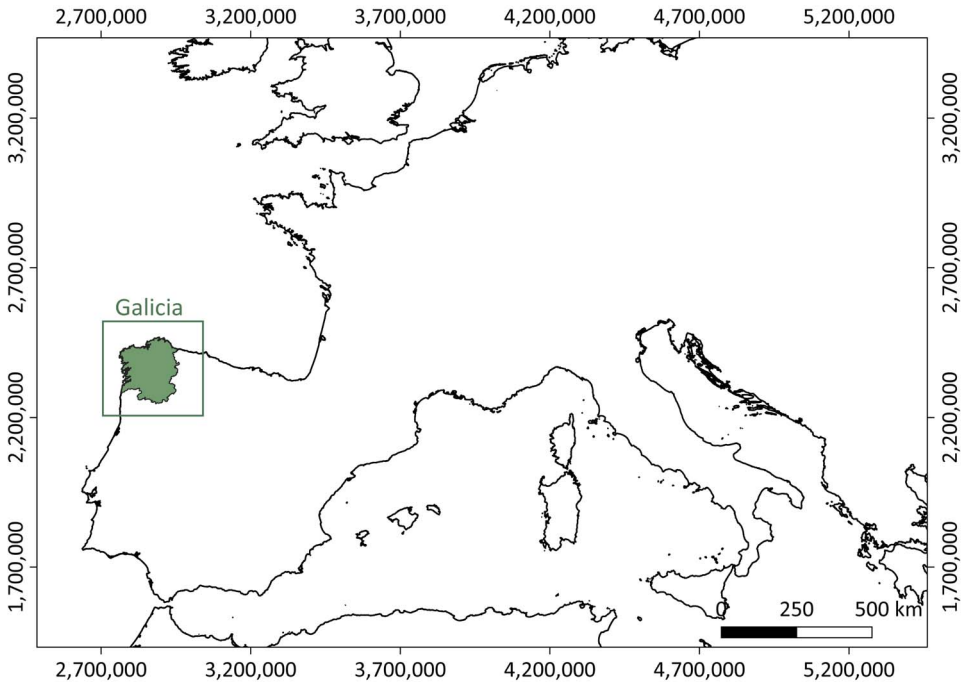

Figure 1 Study area (Galicia, Northwest of Spain).

Table 1 Specifications of spectral bands provided by Sentinel-2 (ESA, 2015b).

Band	Central wavelength (nm)	Bandwidth (nm)	Spatial resolution (m)
Band 1 – Coastal aerosol	443	20	60
Band 2 – Blue	490	65	10
Band 3 – Green	560	35	10
Band 4 – Red	665	30	10
Band 5 – Near Infrared (NIR)	705	15	20
Band 6 – NIR	740	15	20
Band 7 – NIR	783	20	20
Band 8 – NIR	842	115	10
Band 8A – NIR narrow	865	20	20
Band 9 – Water vapor	945	20	60
Band 10 – Shortwave Infrared (SWIR) (cirrus)	1375	30	60
Band 11 – SWIR	1610	90	20
Band 12 – SWIR	2190	180	20

month, an image from the end of the previous month or from the beginning of the following month was selected.

Reference images

Aerial orthorectified images from the Spanish National Plan of Aerial Orthophotography, PNOA by its Spanish acronym (MTMAU, 2021), were used to obtain training and verification datasets. The PNOA images were acquired from the Spanish National Cartographic Institute (IGN) (MTMAU and IGN, 2021). Two sets of open-access images are available: images corresponding to photogrammetric flights performed between the 30th of May and the 1st of September 2017 (PNOA 2017) and images corresponding to photogrammetric flights performed between the 30th of May and the 1st of September 2020 (PNOA 2020). The imagery includes three bands covering the visible spectrum (VIS) (red, green, blue) and a near infrared band (NIR). The Images from 2017 have a spatial resolution of 0.25 m and a georeferencing mean square error of $\leq$0.5 m (MTMAU, 2021). The Images from 2020 have a spatial resolution of 0.15 m and a georeferencing mean square error of $\leq$ 0.20 m (MTMAU, 2021). Google street view (Google Street view, 2021) was also used wherever possible as a complement to the PNOA images.

Methods

From the data presented before, 2 consecutive-year land cover maps were produced and later compared in detail. With this, we aimed to better understand the processes leading to changes from one map to the next with a particular focus on forest changes. The general workflow is presented in Figure 2.

Annual land cover mapping

Two consecutive-year land cover maps were obtained in this study, one map for 2019 (MAP19) and one map for 2020 (MAP20). They were derived following the methodology described by Alonso *et al.* (2021). This method is based on a supervised classification of a set of Sentinel-2 images from a given year and the subsequent aggregation of the classification maps from each satellite image using a set of decision criteria. As a result, a

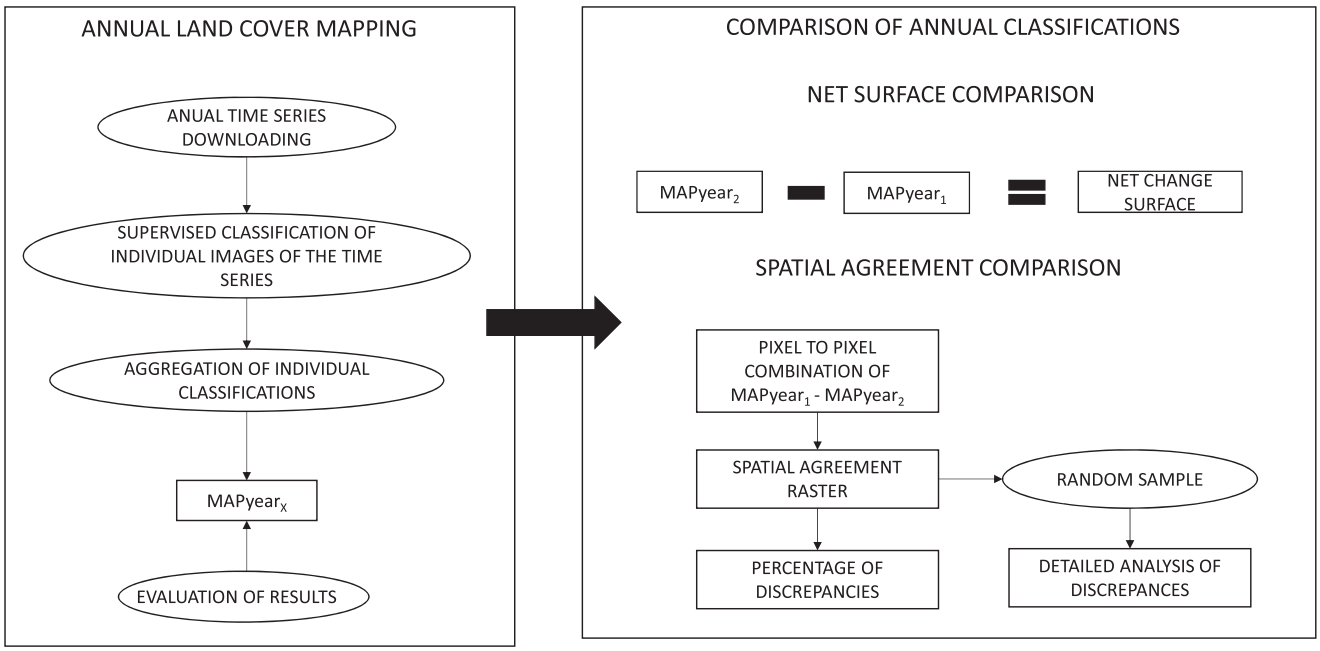

Figure 2 General workflow.

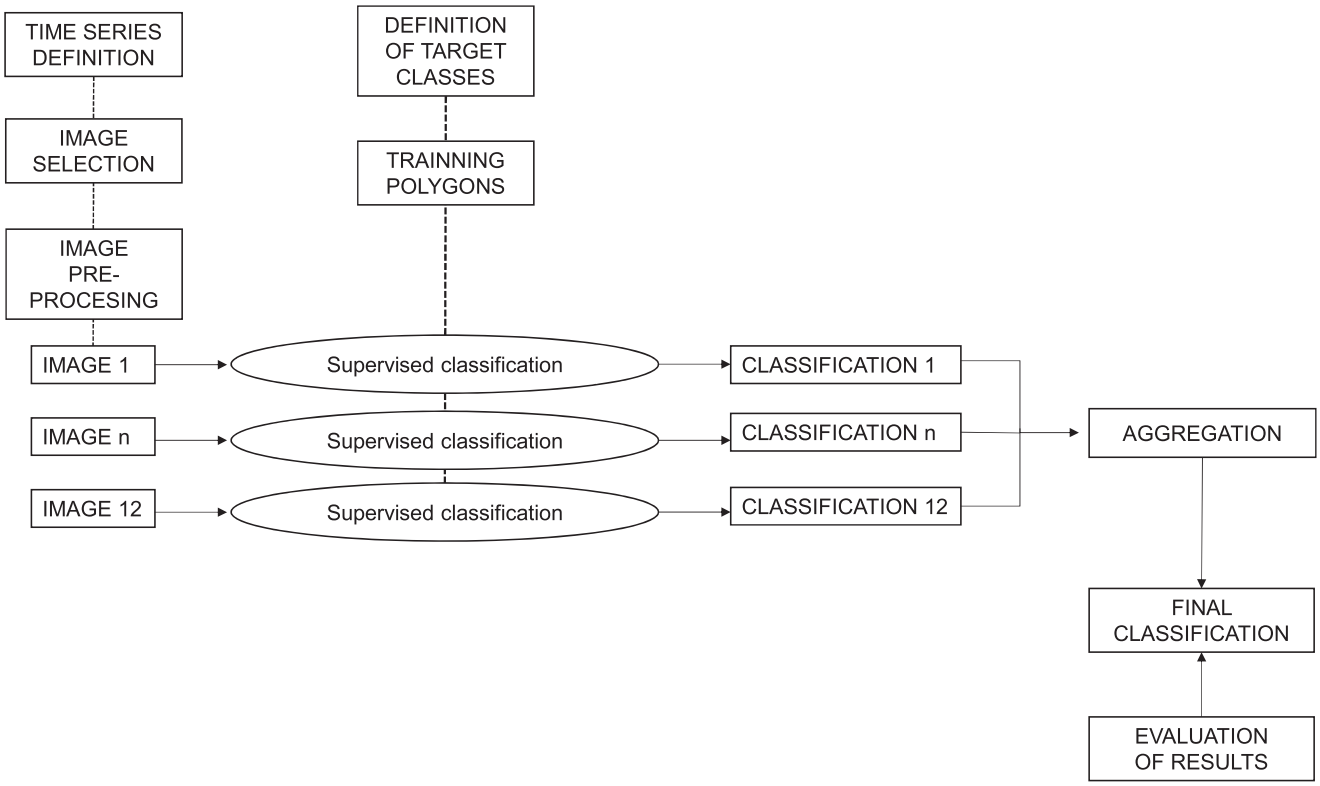

Figure 3 Annual land cover mapping workflow. Source Alonso *et al*. (2021).

single map is obtained that describes the land cover for a given year (Lewinski *et al*., 2017). Figure 3 presents a diagram of the workflow followed (Alonso *et al*., 2021).

The first step in obtaining the annual land cover classifications is the definition of the land cover target classes as presented in Table 2. The same classes were used for both maps.

Table 2 Description of target land cover classes for creating the forest-oriented land cover map of Galicia.

Class	Description
Eucalyptus spp.	Land covered by *Eucalyptus* spp. tress.
Conifers	Land covered by coniferous trees.
Broadleaves	Land covered by broadleaf trees other than *Eucalyptus* spp.
Shrubs	Land covered by non-tree woody vegetation.
Crops and pastures	Land covered by non-woody vegetation.
Bare soil	Land covered by rocks or non-anthropogenic non-vegetated areas.
Anthropogenic areas	Buildings or built-up areas or areas modified by humans, such as mines.
Water	Bodies of water.

A total of 84 images per year, one image per month and seven Sentinel-2 tile covering Galicia, served as input. Once the images were selected and downloaded, the cloudy pixels from each image were masked out of all of the images using the cloud mask provided by the Sentinel-2 Level-2A product.

Training areas were obtained mainly through the photointerpretation of PNOA images 2017, as well as of the occasional use of Google Street view images. A set of polygons for each target class was manually delineated over the whole study region (ROI19). PNOA images from 2020 and Sentinel-2 images dating from 2019 were used as supporting information. They were mostly used to verify that the class in the training area did not change between the years, i.e. an area identified as coniferous forest in the 2017 PNOA image, is also coniferous forest observed in the PNOA 2020 image, whereas no change observed in Sentinel-2 during the whole 2020. This training dataset was used to build the land cover map for 2019 (MAP19).

The training dataset used to create the land cover map for 2020 (MAP20) was obtained by re-inspecting the previous training areas. The 2020 PNOA images (MTMAU, 2021) and Sentinel-2 images dating from 2020 were used; all areas that underwent a change (i.e. forest harvesting) were dropped. They were replaced by a polygon from an area nearby with the same land cover to maintain the number of training polygons per class.

The training areas were distributed throughout the land-area of Galicia. The number of polygons used in the training datasets for each land use class is presented in Table 3, as well as their total area and the minimum size of the defined polygons.

Once the training areas were collected, single-date supervised classifications were conducted for each of the 12 images downloaded for each year, and for each of the seven Sentinel-2 tiles that correspond to Galicia. All supervised classifications were performed using the random forest algorithm (Breiman, 2001) implemented in R using the random Forest package (Liaw and Wiener, 2002). The configuration parameters were set to default (Number of trees: 500). Each random forest model was trained using the training areas from all the tiles that comprise the study area. The predictive bands were all of the Sentinel-2 bands with 10 and 20 m pixel sizes (B02, B03, B04, B05, B06, B07, B08, B8A, B11 and B12). The classification was conducted at a pixel size of 20 m. The 10-m bands of Sentinel-2 were resampled to 20 m using nearest neighborhood interpolation.

Once single date classifications for a year were obtained, they were aggregated following a plurality voting decision criteria (Lewinski *et al*., 2017; Alonso *et al*., 2021). Plurality voting consists of assigning as the ultimate class to each pixel the most common class from among all of the classes identified throughout the time series (Lewinski *et al*., 2017). By doing this, areas that did not have pixel values in a given month (i.e. masked clouds) would be classified according to the most common classification for that pixel in the rest of the months processed. At the end of this process, MAP19 and MAP20 were obtained.

Finally, the maps obtained were cross verified. To perform the cross verification, an independent set of 1674 random points was distributed over the study area. The same set of points was used to verify both years. However, in some cases, the ground truth of some of these points may have changed due to changes produced in the land cover over the course of the 2 years. The ground truth of each point was obtained through photointerpretation of PNOA17 and PNOA20 images (as described in detail in the methods section). Some verification points were discarded as they fell on pixels permanently covered by clouds. This included 18 points for the MAP19 verification and 19 points for MAP20. In addition, 334 verification points were discarded due to the impossibility of obtaining a reliable ground truth through photointerpretation, for example, because the corresponding Sentinel-2 pixel was located in an area with a clearly mixed land-cover. A confusion matrix was built based on the successfully interpreted reference points, and the following metrics were obtained to assess the accuracy of both land cover maps: Overall Accuracy (OA), User's Accuracy (UA), Producer's Accuracy (PA), F-1 Score and Kappa Index. An explanation of each of the accuracy metrics is given in Table 4.

Comparison of annual classifications

Once the results of the consecutive-year classifications were obtained, they were compared to identify changes. This step is in fact the key-contribution of this study as it sought to understanding in detail which changes can be detected reliably, which changes are difficult to identify and the implications for an operational monitoring system. The comparison was performed first in terms of net surface area and secondl in terms of spatial agreement.

The net surface area comparison can be used to provide a general idea of the degree of total land cover change between classifications for the whole study area. The total surface area covered by each class on each year's map was computed. For each class, the total surface area from MAP19 was subtracted from the total surface area from MAP20. It was deemed a positive development of a class in cases where an increment in surface area of a given target class was seen in 2020 and a negative development when the target class's surface area declined in 2020 with respect to its area in 2019.

The spatial agreement comparison aims to locate areas of discrepancy between years and understand the reasons why these discrepancies occur. For this purpose, the maps MAP19 and MAP20 were combined: MAP19 was multiplied by 100 and added to MAP20. This combination was performed using the raster calculator in Qgis (QGIS.org, 2022). Details of this step are presented

Table 3 Summary of training data.

Class	Number of polygons	Total surface 2019 (ha)	Min size of polygons 2019 (m^2)	Total surface 2020 (ha)	Min size of polygons 2020 (m^2)
Eucalyptus spp.	204	667	672	626	672
Conifers	301	981	202	912	202
Broadleaves	199	1292	158	1194	158
Crops and pastures	129	1079	613	1078	613
Shrubs	270	1147	338	1159	338
Bare soils	234	516	76	516	76
Anthropogenic areas	84	698	2686	698	2686
Water	76	2276	364	2276	364

Table 4 Detailed description of accuracy metrics. Source Alonso *et al*. (2021).

Accuracy metric	Definition
Overall Accuracy (OA)	Calculated by summing the number of correctly classified sites (the diagonal of the confusion matrix) and dividing by the number of reference sites. This value indicates the proportion of the reference sites that was correctly classified
Producer's Accuracy (PA)	The result of dividing the number of correctly classified reference points in each category by the total number of reference points for that category. It corresponds to the map accuracy from the point of view of the map maker. It represents how often real features on the ground are correctly shown on the classified map or the probability that a certain land cover of an area on the ground is properly classified.
User's Accuracy (UA)	Computed by dividing the number of correctly classified pixels in each category by the total number of pixels that were classified for that category. This value represents the reliability of the map or the probability that a pixel classified into a given category actually represents that category on the ground.
F-1 Score	Weighted average of the Producer's and User's accuracy.
Kappa Index	Compares the accuracy obtained in the classification to the accuracy that would be obtained randomly. It is calculated as the total accuracy (OA) minus the accuracy that would be obtained by a random classification all divided by one minus the accuracy that would be obtained by a random classification.

in Figure 4. As a result of the process, a new raster was obtained where the digital values included the corresponding 2019 and 2020 classes: the first digit of the new codes corresponded to the 2019 class and third digit to the 2020 class. Wherever the land use for a pixel in MAP19 and MAP20 agreed, the first digit and the third digit of the new raster were the same. However, if the land cover changed from 1 year to the next (for example in cases of harvesting), the first and the third digit were different. From that point on, pixels where the first and the third digit of the new raster did not agree were considered a discrepancy category. In this way, it was possible to know not only the spatial agreement or discrepancy between the two maps but also the direction of these discrepancies.

Once the discrepancy raster was obtained, the percentage of the surface area where annual classifications agree (percentage of agreement) was calculated as well as the percentage of surface area where the classifications disagree. Discrepancies were grouped as follows: (1) tree cover to tree cover, (2) tree cover to non-tree covers, (3) non-tree covers to tree covers and (4) other discrepancies. In this study, the discrepancies that included tree-related classes were then analyzed in detail.

For this, we visually interpreted and analyzed the discrepancy areas to understand the proportion of the discrepancies that was related to any forest disturbance or land cover change and the proportion that was related to classification errors. A total of 30 random points for each discrepancy category was randomly distributed over pixel clumps (pixels that share a side or an edge) of at least six pixels from the same class. This was necessary to simplify the photointerpretation. Each point was inspected in detail to detect whether, from one classification to the next, a real change had occurred (correct discrepancy) or if no real change had occurred (incorrect discrepancy). A change was understood to be any change in the land cover including a decrease in vegetation (i.e. due to timber logging or forest fire) or vegetation recuperation (i.e. reforestation). In areas where a change had in fact occurred, the correctness of the direction of the change was also verified (if the class assigned to that pixel on the MAP20 corresponded to the land cover of that pixel in 2020). The inspection was again based on photointerpretation of PNOA images from 2017 to 2020 and Sentinel-2 images. Subsequently, the following metrics were obtained:

- Percentage of change points: the percentage of the 30 sampled points for each category where any real change had occurred between 2019 and 2020, the percentage of correct discrepancies per discrepancy class.

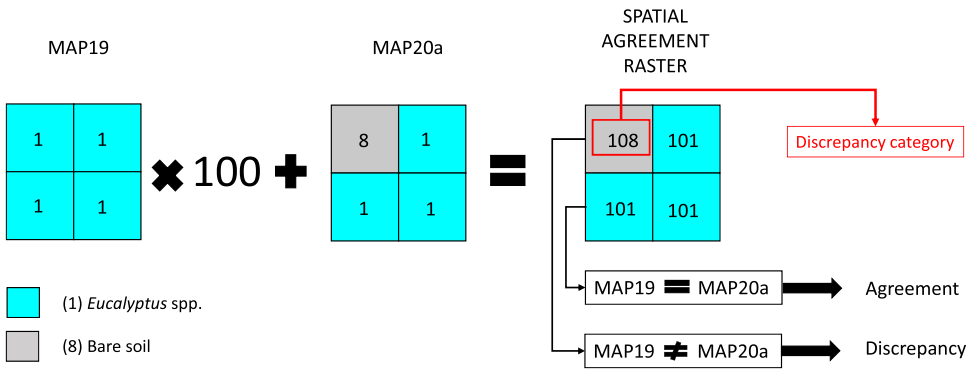

Figure 4 Diagram presenting the combination of MAP19 and MAP20 to obtain the spatial agreement raster which allows for the identification of discrepancy areas and for the detailed study of the direction of these discrepancies.

Table 5 Confusion matrix obtained for MAP19.

Reference/Classified	1	2	3	4	5	6	7	8	T	UA (%)
1	104	11	0	0	0	0	0	0	115	90
2	10	167	5	1	7	0	0	1	191	87
3	8	2	257	9	30	0	0	0	306	84
4	5	1	13	371	21	1	7	0	419	89
5	5	8	2	4	164	0	2	0	185	89
6	0	0	0	2	11	29	13	0	55	53
7	0	0	0	2	2	4	32	0	40	80
8	0	0	0	0	0	0	0	11	11	100
T	132	189	277	389	235	34	54	12	1322	**OA (%)**
PA (%)	79	88	93	95	70	85	59	92	**OA (%)**	86
F-1 Score	0.84	0.88	0.88	0.92	0.78	0.65	0.68	0.96	**KI**	0.82

Classes: *Eucalyptus* spp. (1), Conifers (2), Broadleaves (3), Crops and pastures (4), Shrubs (5), Bare soil (6), Anthropogenic areas (7) and Water (8). Metrics: User's Accuracy (UA), Producer's Accuracy (PA), Overall Accuracy (OA), T: Total, KI: Kappa Index.

- Percentage of correctness of change direction: the percentage of change points (of correct discrepancies) for each category in which the class assigned in MAP20 corresponds to the true land cover of that pixel in 2020.

Results

Annual land cover mapping

The results of the cross verification of MAP19 can be seen in Table 5. A high OA was obtained (86 per cent). UAs and PAs for forestry-related classes were high as well, with most values above 85 per cent. Lower accuracy metrics were obtained for the Bare soil and Anthropogenic classes. As shown in Table 5, these two classes are commonly confused with one another in the classification. MAP20 portrays accurate results as well, as demonstrated in Table 6. The OA was 88 per cent and the forestry-related classes' metrics were all higher than 83 per cent.

Comparison of annual classifications

Once the results of the consecutive-year classifications were obtained, they were compared first with respect to net surface area and second in terms of spatial agreement. We observed a net surface area change of a total of 80 127 ha between the 2019 land cover map and the 2020 land cover map, corresponding to 2.7 per cent of the total land area of Galicia. In Figure 5, the net change between years is shown, categorized by target classes. According to this type of comparison, the class that experienced the greatest net change was Conifers, which occupied 22 944 ha more on MAP20 than on MAP19. Crops and Pastures, as well as Broadleaves, showed large net changes but in the opposite direction. In particular, Broadleaves had a net decrease of 15 343 ha.

However, the results of the spatial agreement comparison show a very different balance of changes when compared with the net comparison. Results are presented in Figure 6, where the following categories are presented:

- Agreement: percentage of the surface area where MAP19 and MAP20 agree.
- Tree–Tree discrepancies: percentage of the surface area where there is a discrepancy between MAP19 and MAP20 but both maps indicate that there is a tree cover.
- Tree-Other/Other-Tree discrepancies: percentage of the surface area where there is a discrepancy between maps MAP19 and MAP20 such that one of the maps indicates that there is

Table 6 Confusion matrix obtained for MAP20.

Reference/ Classified	1	2	3	4	5	6	7	8	T	UA (%)
1	110	9	0	0	0	0	0	0	119	92
2	8	170	2	0	12	0	0	0	192	89
3	6	1	261	3	21	0	1	1	294	89
4	0	2	13	378	22	0	5	0	420	90
5	8	6	1	2	168	0	1	0	186	90
6	0	1	0	4	11	31	17	0	64	48
7	0	0	0	2	1	3	31	0	37	84
8	0	0	0	0	0	0	0	11	11	100
T	132	189	277	389	235	34	55	12	1323	**OA (%)**
PA (%)	83	90	94	97	71	91	56	92	**OA (%)**	88
F-1 Score	0.88	0.89	0.91	0.93	0.80	0.63	0.67	0.96	**KI**	0.85

Classes: *Eucalyptus* spp. (1), Conifers (2), Broadleaves (3), Crops and pastures (4), Shrubs (5), Bare soil (6), Anthropogenic areas (7) and Water (8). Metrics: User's Accuracy (UA), Producer's Accuracy (PA), Overall Accuracy (OA), T: Total, KI: Kappa Index.

Category	S. of absolute change (ha)
NA	-2217
Eucalyptus spp.	7079
Conifers	22944
Broadleaves	-15343
Crops and Pastures	-18166
Shrubs	9185
Bare soil	-4254
Anthropogenic	-83
Water	856
Total	**80127**

Figure 5 Net surface of change between 2019 and 2020 classifications. The NA category represents surfaces permanently covered by clouds.

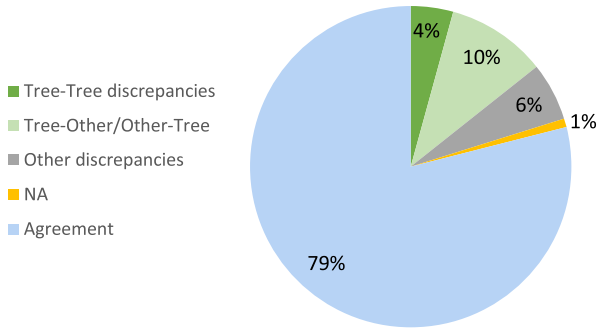

Figure 6 Pie chart presenting the percentage of discrepancies resulting from the spatial agreement analysis of maps MAP19 and MAP20.

a tree-related land cover (Eucalyptus, Conifers or Broadleaves) and the other indicates that there is a non-tree-related land cover.

- Other discrepancies: percentage of the surface area where there is a discrepancy between MAP19 and MAP20 and neither land-cover class indicates a tree-related cover.
- NA: points permanently covered by clouds in either one or both of the maps.

About 20 per cent of the Galician surface area was assigned to a different class in MAP19 than in MAP20. Of these 20 per cent, roughly 6 per cent were related to non-tree classes (for example a discrepancy between Shrubs and Bare soil), whereas the other 14 per cent suggested a tree-related change with 10 per cent corresponding to afforestation or a reduction in vegetation (i.e. an *Eucalyptus* spp. pixel changing to Bare soil as the result of a timber cut or a forest fire). The remaining 4 per cent is attributed to spurious changes between tree covers (i.e. a pixel that was erroneously classified in one of the years).

The detailed results concerning the discrepancy areas are presented in Table 7. They reveal that most pixels in the category 'Tree cover to tree cover discrepancies' represent spurious changes. However, a visual inspection indicated that many of these cases cannot be considered strictly classification errors since they frequently correspond to edge pixels with mixed spectral signatures. In addition, some tree cover to tree cover change pixels corresponded to real changes: logged areas are often assigned to Broadleaves when vegetation such as *Pteridium* spp. or annual grasses appears within the logging year. For example, 50 per cent of the pixels with '*Eucalyptus* spp. to Broadleaves' changes corresponded to harvested Eucalyptus plantations. Furthermore, young *Eucalyptus* spp. plantations that are wrongly classified as Broadleaves (because of recent harvesting) can rapidly change to the *Eucalyptus* spp. class if the crown cover grows dense enough from 1 year to the next. Respective examples can be seen in Figures 7 and 8.

The 'tree cover to non-tree cover discrepancies' category includes changes that implied a reduction in vegetation: any tree-related class in MAP19 that became Shrubs, Crop or pastures, Bare soil or Anthropogenic areas in MAP20. In this case, a great correspondence with real changes was observed. This was especially true when the tree cover was *Eucalyptus* spp. or Conifers: true positives were 97 and 100 per cent, respectively. In general, the metrics were lower when the tree cover was Broadleaves. Only the category 'Broadleaves to Anthropogenic

Table 7 Verification of discrepancies between MAP19 and MAP20.

Discrepancy type	Discrepancy category	Change points (%)	Correctness of change direction (%)
Tree-tree discrepancies	*Eucalyptus* spp. to Conifers	0	-
	Eucalyptus spp. to Broadleaves	50	0
	Conifers to *Eucalyptus* spp.	3	0
	Conifers to Broadleaves	33	0
	Broadleaves to *Eucalyptus* spp.	93	0
	Broadleaves to Conifers	50	0
Tree-Other discrepancies	*Eucalyptus* spp. to Crops or pastures	100	100
	Eucalyptus spp. to Shrubs	33	70
	Eucalyptus spp. to Bare soil	100	100
	Eucalyptus spp. to Anthropogenic areas	100	9
	Conifers to Crops and pastures	100	100
	Conifers to Shrubs	27	88
	Conifers to Bare soil	100	90
	Conifers to Anthropogenic areas	97	0
	Broadleaves to Crops and pastures	40	0
	Broadleaves to Shrubs	3	100
	Broadleaves to Bare soil	37	82
	Broadleaves to Anthropogenic areas	90	11
Other-tree discrepancies	Crops and pastures to Broadleaves	33	10
	Shrubs to *Eucalyptus* spp.	60	94
	Shrubs to Conifers	37	100
	Shrubs to Broadleaves	13	0

Discrepancy category: MAP19 class to MAP20 class. Change points: percentage of the 30 sampled points for each category that exhibited a change from MAP19 to MAP20. Correctness of change direction: percentage of change points for each category in which the class assigned in MAP20 was correct.

areas' corresponded closely, in 90 per cent of cases, with true positives. Finally, a lower correspondence with real changes was found in cases where any of the tree classes changed to Shrubs. The visual inspection of this category revealed that these kinds of discrepancies are often due to thinning. The reduction of the trees' density cover can lead to a situation in which either the spectral signal is indeed dominated by understory shrubs or the sparser tree canopy resembles the spectral signature of shrubs. An example is presented in Figure 9.

Regarding the degree of correctness of the change direction, it is worth noting that it is especially high when *Eucalyptus* spp. and Conifers change to Crops and pastures (100 per cent). However, correctness is quite low, around 10 per cent, in the case of tree cover pixels from 2019 that were then classified as Anthropogenic areas in the 2020 map. It was noticed that these misinterpretations were mainly related to burned areas; an example is provided in Figure 10. After-fire spectral signatures may be more similar to the spectral signature of an impervious surface than to that of another class, such as Bare soil for example, which might have been expected.

Finally, the 'non-tree cover to tree cover category' was found to mostly correspond with tree vegetation recoveries (from shrub to a tree-related category). Plantations at early stages do not have a sufficiently dense canopy cover to be detected as a tree category in the maps and therefore the map only recognizes the spectral answer of the underlying shrubs. But as the plantation species grow a denser canopy cover, they are detected and mapped correctly. An example is shown in Figure 11. However, the rate of true positives was modest in this category: <40 per cent for both Shrubs to Broadleaves and Shrubs to Conifers. A slightly higher correspondence was observed for Shrubs to *Eucalyptus* spp.: 60 per cent. With regard to the correctness of the direction of change, it is worth mentioning that the discrepancy categories implying the recovery of either *Eucalyptus* spp. or Conifers exhibited a high level of correctness: 94 and 100 per cent, respectively.

Discussion

The methodology described in Alonso *et al*. (2021) enabled the creation of annual land cover maps using Sentinel-2 images. High OA metrics and high tree-class-specific and shrubs class accuracy metrics were obtained. These results are in line with the ones reported by Alonso *et al*. (2021) for different dates. The stability of

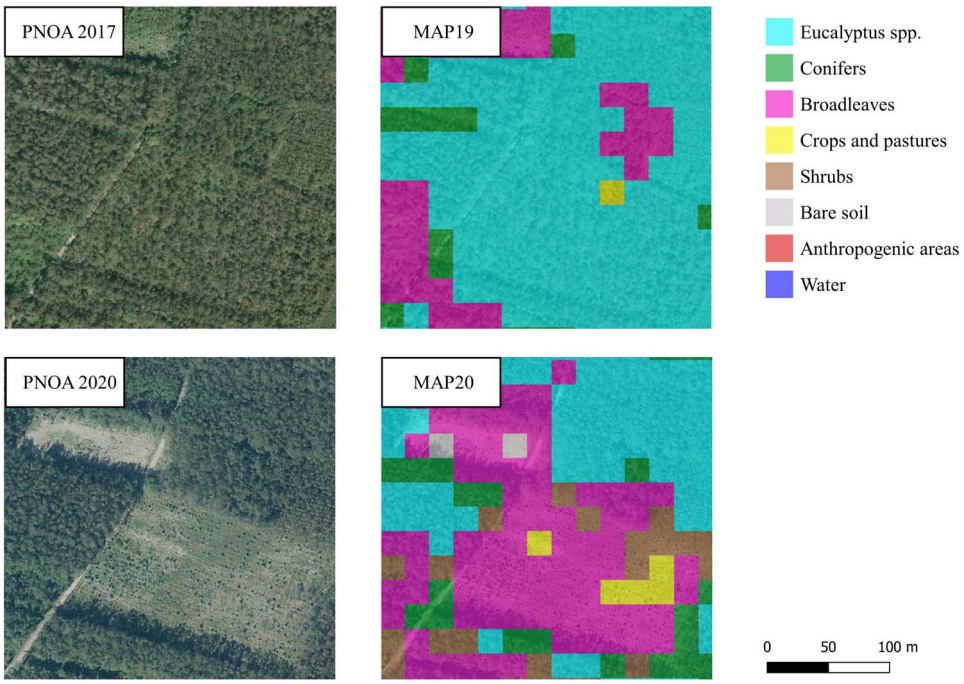

Figure 7 Example of an area erroneously classified as Broadleaves after a *Eucalyptus* spp. harvesting. Reference images: PNOA 2017 (MTMAU, 2021) and PNOA 2020 (MTMAU, 2021).

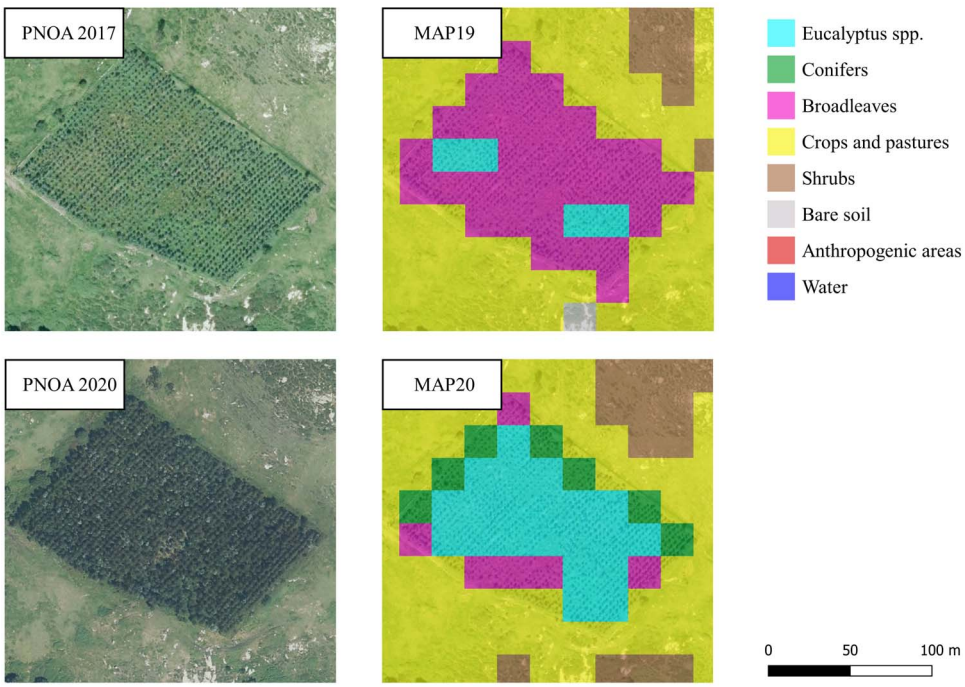

Figure 8 Example of a recently harvested and reforested *Eucalyptus* spp. area erroneously assigned to Broadleaves that is then correctly assigned to Eucalyptus when the trees start to grow. Reference images: PNOA 2017 (MTMAU, 2021) and PNOA 2020 (MTMAU, 2021).

the accuracy metrics both at the overall and the individual class levels over several years attests to the temporal consistency and robustness of this classification method (Tsendbazar *et al*., 2021). This is a matter of great importance when the aim is to capture forest area dynamics through the comparison of land cover maps produced at regular intervals.

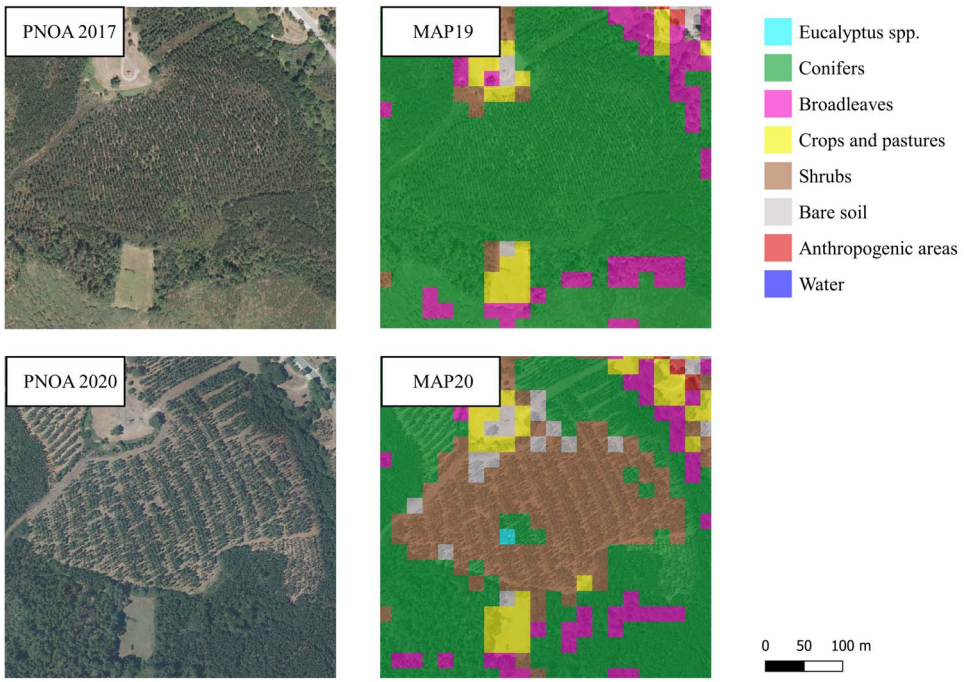

Figure 9 Example of an area erroneously classified as Shrubs after a thinning. Reference images: PNOA 2017 (MTMAU, 2021) and PNOA 2020 (MTMAU, 2021).

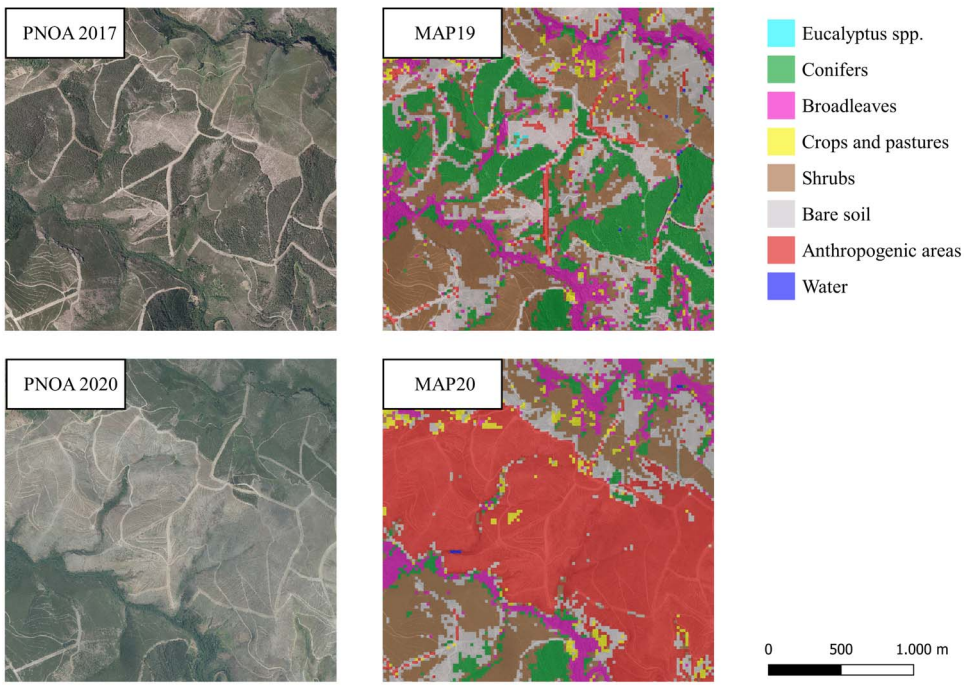

Figure 10 Example of an area assigned to the class Anthropogenic areas after a forest fire event. Reference images: PNOA 2017 (MTMAU, 2021) and PNOA 2020 (MTMAU, 2021).

The two approaches used to compare the consecutive-year classifications in this study yielded notably different results. These differences confirm that reporting the surface of change merely through pixel counting is likely to lead to the wrong conclusions, as previously discussed by Palahí *et al.* (2021), Congalton *et al.* (2014) and Olofsson *et al.* (2013). A much lower percentage of change was found in the net change comparison than in the spatial agreement analysis. This indicates that map errors are at least partially compensated for in the global net change comparison. One of the many examples of

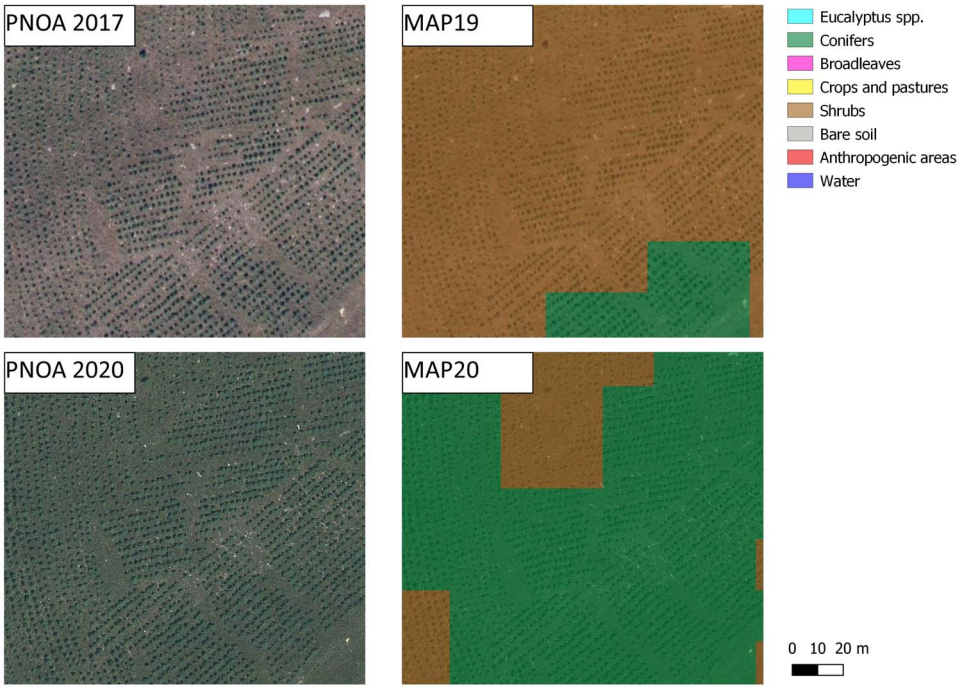

Figure 11 Example of a conifer plantation in an early stage assigned to Shrubs on MAP19 and to Conifers on MAP20. Reference images: PNOA 2017 (MTMAU, 2021) and PNOA 2020 (MTMAU, 2021).

this is that *Eucalyptus* spp. pixels wrongly classified as conifers are compensated for by Conifer pixels wrongly classified as *Eucalyptus* spp. In fact, this effect is also reflected in the confusion matrices. Furthermore, edge effects may also be compensated for within the map.

The spatial comparison of maps from consecutive years revealed the presence of many spurious changes (defined as changes that could have not possibly have occurred in the 2-year time period observed). A detailed visual interpretation of the areas corresponding to these changes showed that a certain number of them correspond to misclassifications (where no change had occurred) or edge pixels. However, some of them were also associated to real changes (true positives). Principally, these real changes included the following scenarios: (a) Pixels changing from *Eucalyptus* spp. to Broadleaves corresponded to logged areas where vegetation such as *Pteridium* spp. or annual grasses had begun to grow; (b) Pixels which changed from Broadleaves to *Eucalyptus* spp. corresponded to young eucalyptus plantations with increasingly closed canopy cover.

One strategy to rectify the spurious changes in maps from consecutive time periods may be to define sets of rules to decide the correct land cover class for pixels affected by these spurious changes (Abercrombie and Friedl, 2015; Zhu *et al*., 2020). Alternatively, a certain inertia could be conferred to the maps by observing data from a time series of longer than 12 months (Wulder *et al*., 2020). Performing seasonal analysis similar to the one performed by Zhao *et al*. (2016) might be also of interest. In this approach, depending on the class in question, the final class assigned to a pixel is either the class identified in a certain season or the class resulting from a plurality voting criteria.

However, these solutions might not solve the problem of inconsistent edge pixels classification from 1 year to the next. In areas like Galicia, where stands are highly fragmented, this can be quite common. Thousands of pixels of 20 m Ground Sampling Distance can be located along the borders of neighboring plantations stocked with different species. Slight variations in the geometry of observation, and mis-registration errors, among other factors, can result in differing land-cover classes assigned to a pixel from 1 year to another (Kukawska *et al*., 2017; Mi *et al*., 2022). One potential solution to deal with edge effect errors may be to transform pixel-based maps into polygon-based maps (Kussul *et al*., 2016; Sohl *et al*., 2017), that is, following an object-based approach. Thus, the pixel information would be used to define the land cover of previously defined vectoral structures, such as cadastral parcels (UKCEH, 2020). This approach could aid, as well, in the analysis of forest evolution since it allows for changes to be studied in relatively permanent units that also tend to be have a direct relation to the scale at which these changes occurs (Sohl *et al*., 2017). However, disturbances and harvesting can also occur at a sub-parcel level and hence this approach may also result in polygons with mixed land cover classes.

In the spatial comparison approach, the discrepancy category 'tree to others' proved to be highly reliable, especially when it involved *Eucalyptus* spp. and Conifers. This category could be useful for forest monitoring purposes since it could be used as the basis for a harvesting alert system which would identify eligible candidates to check through field work or high resolution remote sensing data. Such a system could be useful in regions with a highly active forestry sector, where the verification of all declared harvests is otherwise impossible because cutting is constant and harvestings are continual and greatly dispersed.

The visual inspection of the tree-to-other discrepancy areas showed that some areas classified as Shrubs, Crops and pastures or Bare soil on the maps met the criteria for standard definitions of forests (FAO, 2018; Official Journal of the European Union, 2018). For example, some areas that have been logged are classified as bare soil when in reality they are merely temporally unstocked areas expected to regenerate. Therefore, if national and international forest monitoring is to be conducted according to the requirements of the FAO, a system based on annual land cover maps might not be adequate for monitoring the actual true forest area. Solutions like the ones presented by Wulder *et al.* (2020), that take several years data into consideration, might be more appropriate. This temporal inertia may also be necessary to define and analyze the direction of the changes that properly represents forest dynamics.

In summary, this study discussed some strengths and limitations of comparing annual land cover maps for forest monitoring purposes. The maps, as well as a detailed error analysis, such as the one conducted in this study, could be used as input in more specific forest dynamics analysis (Estes *et al*., 2017). For example, information about the reduction or increase in broadleaf forest cover can be helpful in assessing the state of conservation of an area because broadleaf forests serve as habitats for certain endangered and protected animals which do not live in pine or eucalyptus plantations. In such scenarios, awareness of the mapping errors surrounding Eucalyptus plantations and edge pixels can help to correctly interpret results with respect to the destruction or evolution of these animals' habitats.

Conclusion

In this study, 2 consecutive-year land cover maps were used to analyze tree-related land cover changes in a study area characterized by a high frequency of land cover changes, presence of fast-growing species and a high level of stand fragmentation. The land-cover maps were obtained from Sentinel-2 satellite images using a multitemporal approach based on a random forest classifier. Both maps showed high accuracies, a testament to the consistency of the classification methodology.

However, although individually obtained accuracies were high, a great deal of spurious changes (changes that could not have taken place within the timeframe analyzed) were observed . A detailed analysis of selected areas led to a greater understanding of the processes underlying these spurious changes. For example, a change from shrubs to broadleaf stands frequently corresponded to very young Eucalyptus plantations whose canopy was starting to close. Meanwhile, changes from a forest category to shrubs often corresponded to thinning activities. Understanding these processes that lead to misclassifications is key when seeking to enhance forest monitoring through land cover map comparisons. One of such improvements could be to automatically correct pixels affected by spurious changes by assigning the class which is most likely to be the correct class of a given spurious change and then verifying the assignment using data of subsequent years.

The results shown in this study will be used to advance in the design of a workflow to operationally monitor and report annual forest changes and analyze forest evolution across the whole region of Galicia. The approach presented could also be useful to better understand forest change dynamics of other regions with a similar environmental and management contexts.

Data availability statement

The data underlying this article were accessed from https://scihub.copernicus.eu/dhus/#/home. The derived data generated in this research will be shared upon reasonable request to the corresponding author.

Author contribution

Laura Alonso: Conceptualization, Data curation, Formal analysis, Funding acquisition, Investigation, Methodology, Software, Validation, Visualization, Writing – original draft, Writing – review and editing.
Andrés Rodríguez: Data curation, Formal analysis, Investigation, Methodology, Software, Validation.
Juan Picos: Conceptualization, Funding acquisition, Methodology, Project administration, Resources, Supervision, Writing – review and editing.
Julia Armesto: Conceptualization, Funding acquisition, Methodology, Project administration, Supervision, Validation, Writing – review and editing.

Conflict of Interest statement

None declared.

Funding

This research is part of the 'Continuous forestry inventory of Galicia' project funded by the Administration of Rural Areas of the Government of Galicia under grant 2020CONVINVENTARIOFORESTALR002. It is also supported by an FPU grant from the Spanish ministry of Sciences, Innovation and Universities under grant FPU19/02054. Additional support comes from the PID2019- 111581RB-I00 project PALEOINTERFACE: STRATEGIC ELEMENT FOR THE PREVENTION OF FOREST FIRES, DEVELOPMENT OF MULTISPECTRAL AND 3D ANALYSIS METHODOLOGIES FOR INTEGRATED MANAGEMENT, of the Spanish Ministry of Sciences, Innovation and Universities. In addition, it benefits from the aid of the Teaching Innovation Group 'ODS Cities and Citizenship' of the University of Vigo. Funding for open access charge: Universidade de Vigo/CISUG.

References

Abercrombie, S. and Friedl, M. 2015 Improving the consistency of multitemporal land cover maps using a hidden Markov model. *IEEE Trans. Geosci. Remote Sens.* **54**, 1–11. 10.1109/TGRS.2015.2463689.

Alonso, L., Picos, J. and Armesto, J. 2021 Forest Land cover mapping at a regional scale using multi-temporal Sentinel-2 imagery and RF models. *Remote Sens.* **13**, 2237. https://doi.org/10.3390/rs13122237.

Arenas, S., Rodríguez-Soalleiro, R. and Diaz-Balteiro, L. 2019 *Turno óptimo de Eucalyptus nitens en Galicia introduciendo la fiscalidad en el análisis*. XII Congreso de Economía Agraria.

Breiman, L. 2001 Random forests. *Mach. Learn.* **45**, 5–32. https://doi.org/10.4236/ijis.2019.94007.

Congalton, R.G., Gu, J., Yadav, K., Thenkabail, P. and Ozdogan, M. 2014 Global land cover mapping: a review and uncertainty analysis. *Remote Sens.* **6**, 12070–12093. https://doi.org/10.3390/rs61212070.

ESA (European Space Agency) 2015a *Sentinel-2*. https://www.esa.int/Space_in_Member_States/Spain/SENTINEL_2 (accessed on 23 July, 2021)

ESA (European Space Agency) 2015b *ESA Standard Document—Sentinel-2 User Handbook*. https://sentinels.copernicus.eu/web/sentinel/user-guides/document-library/ /asset_publisher/xlslt4309D5h/content/sentinel2-user-handbook (accessed on 23 July, 2021).

ESA (European Space Agency). *12odelling12 and European Comission. Copernicus Open Access Hub*. https://scihub.copernicus.eu/dhus/#/home (accessed on 23 July, 2021).

Estes, L., Chen, P., Debats, S., Evans, T., Ferreira, S., Kuemmerle, T., *et al*. 2018 A large-area, spatially continuous assessment of land cover map error and its impact on downstream analyses. *Glob. Chang. Biol.* **24**, 322–337. https://doi.org/10.1111/gcb.13904.

European Commission. *Paris Agreement*, 2021 https://ec.europa.eu/clima/policies/international/negotiations/paris_en (accessed on 21 July, 2021).

FAO. 2018 *Global Forest Resources Assessment 2020. Terms and Definitions*. Forest Resources Assessment Working Paper, FAO, 188, Rome.

FAO 2020 Better Data, Better Decisions – Towards Impactful Forest Monitoring. Forestry Working Paper 16. FAO. https://doi.org/10.4060/cb0437en.

FAO. 2021. *REDD++ Reducing Emissions from Deforestation and Forest Degradation*. http://www.fao.org/redd/en/ (accessed on 21 July, 2021).

Gilani, H., Naz, H., Arshad, M., Nazim, K., Akram, U., Abrar, A., *et al*. 2020 Evaluating mangrove conservation and sustainability through spatiotemporal (1990-2020) mangrove cover change analysis in Pakistan. *Estuar. Coast. Mar. Sci.* **249**, 107128. https://doi.org/10.1016/j.ecss.2020.107128.

Google Street View. 2021. https://www.google.es/intl/es/streetview/ (accessed on 23 July, 2021).

Inglada, J., Vincent, A., Arias, M., Tardy, B., Morin, D. and Rodes, I. 2017 Operational high resolution land cover map production at the country scale using satellite image time series. *Remote Sens.* **9**, 95. https://doi.org/10.3390/rs9010095.

Ji, Q., Liang, W., Fu, B., Zhang, W., Yan, J., Lü, Y., *et al*. 2021 Mapping land use/cover dynamics of the yellow river basin from 1986 to 2018 supported by google earth engine. *Remote Sens.* **13**, 1299. https://doi.org/10.3390/rs13071299.

Jin, S., Yang, L., Zhu, Z. and Homer, C.A. 2017 Land cover change detection and classification protocol for updating Alaska NLCD 2001 to 2011. *Remote Sens. Environ.* **195**, 44–55. https://doi.org/10.1016/j.rse.2017.04.021.

Junta de Castilla y León. 2021. *Mapa de cultivos y superficies naturales*. http://mcsncyl.itacyl.es/ (accessed on 21 July, 2021).

Kang, J., Wang, Z., Sui, L., Yang, X., Ma, Y. and Wang, J. 2020 Consistency analysis of remote sensing land cover products in the tropical rainforest climate region: a case study of Indonesia. *Remote Sens.* **12**, 1410. https://doi.org/10.3390/rs12091410.

Kukawska, E., Lewiński, S., Krupiński, M., Malinowski, R., Nowakowski, A., Rybicki, M., Kotarba, A. 2017 Multitemporal Sentinel-2 data—remarks and observations. In *Proceedings of the 2017 9th International Workshop on the Analysis of Multitemporal Remote Sensing Images (MultiTemp)*, IEEE, Brugge, Belgium, 27–29 June 2017, pp. 2–5.

Kussul, N., Lemoine, G., Gallego, F.J., Skakun, S.V., Lavreniuk, M. and Shelestov, A.Y. 2016 Parcel-based crop classification in Ukraine using landsat-8 data and sentinel-1A data. *IEEE J. Select. Topics Appl. Earth Observ. Remote Sens.* **9**, 2500–2508. https://doi.org/10.1109/JSTARS.2016.2560141.

Levers, C., Verkerk, H., Müller, D., Verburg, P., Butsic, V., Leitão, P., *et al*. 2014 Drivers of forest harvesting intensity patterns in Europe. *For. Ecol. Manag.* **315**, 160–172. https://doi.org/10.1016/j.foreco.2013.12.030.

Lewinski, S., Nowakowski, A., Malinowski, R., Rybicki, M., Kukawska, E., Krupinski, M. 2017 Aggregation of Sentinel-2 time series classifications as a solution for multitemporal analysis. In *Proceedings Volume 10427, Image and Signal Processing for Remote Sensing XXIII, SPIE Remote Sensing*. Warsaw, Poland. https://doi.org/10.1117/12.2277976

Liaw, A. and Wiener, M. 2002 Classification and regression by random forest. *R News* **2**, 18–22.

Meteogalicia. https://www.meteogalicia.gal/web/inicio.action (accessed on 21 July, 2021)

Mi, J., Liu, L., Zhang, X., Chen, X., Yuan, G., Xie, S. 2022 Impact of geometric misregistration in GlobeLand30 on land-cover change analysis, a case study in China. *J. Appl. Remote. Sens.* **16**(1), 014516. https://doi.org/10.1117/1.JRS.16.014516

MITERD (Ministerio para la Transición Ecológica y el Reto Demográfico). 2018 *Anuario de estadística forestal*. https://www.mapa.gob.es/es/desarrollorural/estadisticas/aef_2018_documentocompleto_tcm30-543070.pdf (accessed on 21 July, 2021).

MTMAU (Ministerio de Transporte Movilidad y Agenda Urbana) and IGN (Instituto geográfico Nacional). 2021 *Centro de Descargas. Centro Nacional de Información Geográfica*. http://centrodedescargas.cnig.es/CentroDescargas/index.jsp (accessed on 23 July, 2021).

MTMAU (Ministerio de Transporte Movilidad y Agenda Urbana). 2021 *Plan Nacional de Ortofotografía Aérea (PNOA)*. https://pnoa.ign.es/ (accessed on 23 July, 2021).

Mundialis. 2019 *Germany 2019 – Land cover based on Sentinel-2 data*. https://www.mundialis.de/en/deutschland-2019-landbedeckung-auf-basis-von-sentinel-2-daten/ (accessed on 21 July, 2021).

Official Journal of the European Union. 2018 *Regulation (EU) 2018/841 of the European Parliament and of the Council of 30 May 2018 on the inclusion of greenhouse gas emissions and removals from land use, land use change and forestry in the 2030 climate and energy framework, and amending Regulation (EU) No 525/2013 and Decision No 529/2013/EU*.

Olofsson, P., Foody, G., Stehman, S. and Woodcock, C. 2013 Making better use of accuracy data in land change studies: estimating accuracy and area and quantifying uncertainty using stratified estimation. *Remote Sens. Environ.* **129**, 122–131. https://doi.org/10.1016/j.rse.2012.10.031.

Palahí, M., Valbuena, R., Senf, C., Acil, N., Pugh, T.A.M., Sadler, J., *et al*. 2021 Concerns about reported harvests in European forests. *Nature* **592**, E15–E17. https://doi.org/10.1038/s41586-021-03292-x.

Pan, Y., Birdsey, R., Fang, J., Houghton, R., Kauppi, P., Kurz, W., *et al*. 2011 Large and persistent carbon sink in the world's forests. *Science (New York, N.Y.)* **333**, 988–993. https://doi.org/10.1126/science.1201609.

QGIS.org. 2022 *QGIS Geographic Information System*. QGIS Association. http://www.qgis.org (accessed on 31 March, 2022).

Sánchez, González, R., Gómez Viñas, P., Orro, M.L. and Estévez Rial, C. 2013 Phenological observations in Galicia (Observaciones Fenológicas en Galicia). *Calendar. Meteorol.* 291–297.

Spanish government. 2011 *Ministerio de Hacienda*. Sede Electrónica del Catastro. https://www.sedecatastro.gob.es (accessed on 23 July, 2021).

Tolosana, E., Diaz-Balteiro, L. and Lobo-Huici, E. 2017 *Estudio del turno óptimo de Eucalyptus globulus en el norte de España,* VII Congreso Forestal Español, SECF, ISBN 978-84-941695-2-6.

Tsendbazar, N., Herold, M., Li, L., Tarko, A., de Bruin, S., Masiliunas, D., *et al*. 2021 Towards operational validation of annual global

land cover maps. *Remote Sens. Environ.* **266**, 112686. https://doi.org/10.1016/j.rse.2021.112686.

S2GLC. *Map of Europe. Land Cover Map of Europe 2017*. http://s2glc.cbk.waw.pl/extension (accessed on 21 July, 2021).

Sohl, T., Dornbierer, J., Wika, S., Sayler, K., Quenzer, R. 2017. Parcels versus pixels: modelling agricultural land use across broad geographic regions using parcel-based field boundaries. *J. Land Use Sci.* **12**(4), 197–217. https://doi.org/10.1080/1747423X.2017.1340525.

UKCEH (UK Environmental Information Data Centre). 2020 *Land Cover Map 2020*. https://catalogue.ceh.ac.uk/documents/14a9ec05-071a-43a5-a142-e6894f3d6f9d (accessed on 31 March, 2022).

United Nations. 2021 *Sustainable development goals*. https://www.un.org/sustainabledevelopment/ (accessed on 21 July, 2021).

Wickham, J., Homer, C., Vogelmann, J., McKerrow, A., Mueller, R., Herold, N., *et al.* 2014 The Multi-Resolution Land Characteristics (MRLC) Consortium — 20 years of development and integration of USA National Land Cover Data. *Remote Sens.* **6**, 7424–7441. https://doi.org/10.3390/rs6087424.

World Resources Institute. 2022 *Global Forest Watch*. https://www.globalforestwatch.org/ (accessed on 31 March, 2022).

Wulder, M.A., Coops, N.C., Roy, D.P., White, J.C. and Hermosilla, T. 2018 Land Cover 2.0. *Int. J. Remote Sens.* **39**, 4254–4284. https://doi.org/10.1080/01431161.2018.1452075.

Wulder, M., Hermosilla, T., Stinson, G., Gougeon, F.A., White, J.C., Hill, D.A., *et al.* 2020 Satellite-based time series land cover and change information to map forest area consistent with national and international reporting requirements. *Forestry* **93**, 331–343. https://doi.org/10.1093/forestry/cpaa006.

Xunta de Galicia. 2016 *1ª revisión del plan forestal de galicia. Documento diagnóstico del monte y el sector forestal gallego*. https://mediorural.xunta.gal/sites/default/files/temas/forestal/plan-forestal/1_revision_plan_forestal_cast.pdf (accessed on 21 July, 2021).

Xunta de Galicia. 2021 *Sistema de indicadores da administración dixital*. Producción forestal. https://indicadores-forestal.xunta.gal/portal-bi-internet/dashboard/Dashboard.action?selectedScope=OBSFOR_BI_A02_INT&selectedLevel=OBSFOR_BI_2_INT.L0&selectedUnit=12&selectedTemporalScope=2&selectedTemporal=31/12/2020 (accessed on 03 December, 2021).

Zhao, Y., Feng, D., Yu, L., Wang, X., Chen, Y., Bai, Y., *et al.* 2016 Detailed dynamic land cover mapping of Chile: accuracy improvement by integrating multi-temporal data. *Remote Sens. Environ.* **183**, 170–185.

Zhu, L., Shi, R. and Peng, S. 2020 Removing land cover spurious change by geo-eco zoning rule base. *ISPRS - Int. Arch. Photogr. Remote Sens. Spatial Inform. Sci.* **XLII-3/W10**, 677–683. https://doi.org/10.5194/isprs-archives-XLII-3-W10-677-2020.